



PULSAR BRAKING INDEX DUE TO MAGNETIC QUADRUPOLE RADIATION

By
Selemawit Mehari

A THESIS SUBMITTED TO
THE DEPARTMENT OF PHYSICS

PRESENTED IN PARTIAL FULFILLMENT OF THE REQUIREMENTS
FOR THE DEGREE OF MASTER OF SCIENCE

ADDIS ABABA UNIVERSITY
ADDIS ABABA, ETHIOPIA
JUNE 2014

ADDIS ABABA UNIVERSITY
SCHOOL OF GRADUATE STUDIES

This is to certify that the thesis prepared by **Selemawit Mehari**, entitled “**Pulsar Braking Index Due To Magnetic Quadrupole Radiation**” and submitted in partial fulfillment of the requirements for the degree of **Master of Science**. complies with the regulations of the University and meets the accepted standards with respect to originality.

Signed by the Examining Committee:

Examiner: _____ Signature: _____ Date: _____

Examiner: _____ Signature: _____ Date: _____

Advisor: _____ Signature: _____ Date: _____

Abstract

This thesis intends to show that the strong correlation observed between the braking indices (n) and the slowing down age (τ) of pulsars with alignment and counter alignment. We will calculate the braking index of young pulsar which is crab pulsar is less than 3 by using the braking mechanisms, electromagnetic and gravitational radiations, & the braking index for quadrupole radiation is equal to 5, and to show the ratio between the gravitational and electromagnetic contributions to the pulsar spin down rate its present values are always less than one.

Acknowledgements

First of all, I would like to thank Almighty God for letting me accomplish this study. Secondly, I would like to express my heart felt gratitude to my advisor Dr. Legesse Wetro, for his invaluable advices, continuous support and friendly approach through out this research. I am also thankful to kidanemariam Abadi for their support, useful discussions and constructive criticism. It is pleasure to thank the Astrophysics group for their contribution in strengthening the group and the completion of this paper. Also, I would like to express my special thanks to my parents, for providing me all their best. I would like to acknowledge the physics department of Addis Ababa University for providing materials to carry out my thesis. I would also like to thank W/ro. Tsilat, secretary of the department, for printing this thesis and cooperation she showed during my stay in the department.

Addis Ababa University
June,2014

Selemawit Mehari

Table of Contents

Abstract	iii
Acknowledgements	iv
Table of Contents	v
List of Figures	vi
Introduction	1
1 Pulsars	3
1.1 Definition	3
1.2 Discovery of Pulsars	4
1.3 Formation of Pulsars	4
1.4 Pulsars as Radio Sources	6
2 Braking Index Diagnostics	8
2.1 Braking Index of Pulsar	8
2.2 Alignment and Counteralignment	10
2.3 Slowing-down noise	15
3 Braking Mechanisms of Pulsars	18
3.1 Electromagnetic Radiation	18
3.2 Electromagnetic plus Gravitational Radiation	21
3.2.1 Ratio of energy loss due to gravitational versus electromagnetic radiation	26
4 Discussion and Conclusion	28
References	30

List of Figures

1.1	A pulsar is a rotating, highly magnetized neutron star. A radio beam centered on the magnetic axis is created in some distance to the pulsar. The tilt between the rotation and magnetic axes makes the pulsar in effect a cosmic light house when the beam sweeps around in space. . . .	7
2.1	Braking Index Vs slowing-down-Age Correlation. Plotted is the logarithm of the absolute value of the braking index against the logarithm of age. Also shown are the theoretical curves for alignment (solid lines), those for counteralignment (dotted lines) and that given by the Standard $n = 3$ model (dashed line).The alignment curves are labelled by alignment timescales, τ_a ; different values of the field decay timescale, τ_B , in the range $(10^6 - 10^7)$ year make no visible difference for these curves.The counteralignment curves are labelled by τ_B , different values of the counteralignment timescale, τ_c , in the range $(10^3 - 10^7)$ year make little visible difference for these curves.Filled circles:measurements quoted with error bars as shown. Open circles: measurements quoted without error bars. . . .	14
2.2	Same as Fig. 2.1, but comparing the observed braking indices (circles) with those expected from slowing-down noise (triangles). Filled circles: measurements quoted with error bars as shown. open circles: measurements quoted without error bars. For vela, the slowing down noise component itself has an uncertainty as shown (Downs 1981). Also shown are the noise-band (the area between the two solid lines which corresponding to the maximum and minimum values of τ_R in Table 2) and the relation $ n - (\frac{\tau}{10^5} year)^2$ (dashed line) which describes most pulsars adequately.	17
3.1	$Y(n) = \frac{\hat{\Omega}_{gw}}{\Omega_{em}}$ as a function of the braking index n for different values of the electromagnetic braking index n_{em} . n_{em} varies in the range $[1, 3]$ with step 0.2.	25

Introduction

It is believed that all neutron stars rotate, quite rapidly. As a result, some observations of neutron stars yield a "pulsed" emission signature. So neutron stars are often referred to as pulsating stars (or PULSARS), but differ from other stars that have variable emission.

Whether the magnetic and rotation axes of pulsars align or counter align with age has been a much debated but unsettled point. The many theoretical calculations performed to date give widely different results. (Davis & Goldstein 1970)[1] and (Michel & Gold w.1970)[2] showed that for a perfectly conducting spherical star, the two axes align on a braking time scale, a result that can be generalized to a fluid body whose rotation deformation follows the instantaneous rotation axis (Macy 1974)[3].

The observational situation is uncertain. The presence of a strong inter pulse in the crab was used to argue that rotation and magnetic axis were nearly orthogonal in this pulsar (Rad,h. & cooke 1969)[4].

Measurements of the second derivative of the pulsar period, \ddot{p} (or equivalently, the frequency second derivative $\ddot{\Omega}$, or the braking index, $n = \frac{\Omega\ddot{\Omega}}{\dot{\Omega}^2}$) provide us with another potential diagnostic tool for testing alignment or counter alignment. In this paper, We introduce the plot of the braking index, n versus the slowing down age, $\tau = \frac{p}{\dot{p}}$ as a powerful way of using the second derivative data.

From the timing measurements We deduce that radio pulsars are subject to a systematic secular spin down. The standard formula for pulsar spin down is

$$\dot{\Omega} = -k\Omega^n \tag{0.0.1}$$

The quantity $I\dot{\Omega}$, I being the star moment of inertia with respect to its rotation axis, is the torque acting on the star. We will refer to k , following (Allen & Horvath 1997)[5], as the "torque function" and the braking index n both depend on the mechanism which is at work. For instance, n is equal to 3 for pure magnetic dipole radiation and n is equal to 5 for gravitational radiation. In practice, however the measured value of the braking indices for dipole radiation are less than the canonical value, 3 for most known pulsars:

The braking index of the known pulsars are not dominated by timing noise (Lyne et al. 1993[6] ; Boyd et al. 1995[7] ; Kaspi et al. 1994[8] ; Lyne et al. 1996[9]):

$$Crab : n = 2.51 \pm 0.01$$

$$PSR0540 - 69 : n = 2.28 \pm 0.02$$

$$PSR1509 - 58 : n = 2.83 \pm 0.001$$

$$Vela : n = 1.4 \pm 0.2$$

A much more realistic hypothesis is that in a pulsar both electromagnetic and gravitational torques work to produce the observed spin down. We will show how from this assumption the observed braking indexes can be derived and at the same time, how new more tightening upper limits on the pulsar ellipticity are obtained. The plan of the thesis is as follow. In chapter 1, contains review about creation and distinctive properties of pulsars. In chapter 2, I try to drive the braking index of pulsars is inconsistent with counter alignment between their rotation and magnetic axes, the magnetic field and slowing down age τ of the young pulsar which is crab pulsar. In chapter 3, I give the main relations relative to the electromagnetic braking mechanism and described by combining electromagnetic and gravitational mechanisms which could produce the observed braking indexes.

Finally, In section 4 discussion and conclusion are included.

Chapter 1

Pulsars

1.1 Definition

Pulsars are highly magnetized, rotating neutron stars which emit a narrow radio beam along the magnetic dipole axis. As the magnetic axis is inclined to the rotation axis, the pulsar acts like a cosmic light-house emitting a radio pulse that can be detected once per rotation period when the beam is directed toward Earth. The stability of the pulse period is similar to that achieved by the best terrestrial atomic clocks. Using these astrophysical clocks by accurately measuring the arrival times of their pulses, a wide range of experiments is possible. For most of these it is not necessarily important how the radio pulses are actually created. We will consider some of the basic pulsar properties below.

Pulsars are born in supernova explosions of massive stars. Created in the collapse of the stars 'core' neutron stars are the most compact objects next to black holes. The masses of pulsars are typically around $1.35 \pm 0.04 M_{\odot}$ [10] although this range has been expanded recently from $\sim 1.2 M_{\odot}$ to $2.1 M_{\odot}$. Modern calculations for different equations of state produce results for the size of a neutron star which are quite similar to the very first calculations by Oppenheimer & Volkov [11], i.e. a diameter of about 20 km. Such sizes are consistent with independent estimates derived from X-ray light-curves and luminosities of pulsars (e.g. [12]).

Pulsars emit electromagnetic radiation and, in particular, magnetic dipole radiation as they essentially represent rotating magnets. Assuming that this is the dominant process of loss in rotational energy and hence responsible for the observed

increase in rotation period, P , described by \dot{p} , we can equate the corresponding energy output of the dipole to the loss rate in rotational energy. We obtain an estimate for the magnetic field strength at the pulsar (equatorial) surface from

$$B \sin \alpha = 3.2 \times 10^{19} \sqrt{\dot{p} p} \quad (1.1.1)$$

with P measured in s and \dot{p} s^{-2}

1.2 Discovery of Pulsars

In 1934,[13] only two years after the discovery of the neutron, the existence of neutron stars was proposed by astrophysicists, (Baade & Zwicky)[14] . They suggested that neutron stars would be about 10 Km in diameter and would be formed in a supernova. Then, in 1967, Pacini[15] proposed that the crab Nebula was highly magnetised, rotating and emitting electromagnetic radiation. In effect, what we know to be a pulsar. These theories were later confirmed by Jocelyn Bell, Antony Hewish[16] and colleagues in 1968 when they discovered the first pulsar.

At the time they were working on a large radio telescope, observing inter planetary scintillation and they noticed that, aside from the usual scintillation and man-made interference, there was some highly periodic "scruff".

further observation and analysis of this "scruff" showed that the signal kept sidered time which suggested that it was of extraterrestrial origin. Several possible explanations were offered, including that the signal was generated by another civilisation, but it is now almost universally agreed that pulsars are rotating neutron stars which appear to pulsate as their radiation beams the earth.

1.3 Formation of Pulsars

Most of the stars in the universe have similar properties to our sun. Typically they are about 1 million km in diameter and fuelled by hydrogen. Because of their extreme temperature, this hydrogen fuel burns to form helium, making them just like a massive hydrogen bomb.

After about 10 billion years, a star's hydrogen runs out. When this happens the star swells to about three hundred times its normal size and gently pushes out its furthest layers to form a glowing ring known as a planetary nebula. The center of the original star remains intact and becomes a white dwarf, which is a very small, dense star. Initially very hot (about 1 million degrees), it eventually cools down to float relatively inactively throughout the universe.

One in every hundred stars are different. These are massive stars and are destined to end their lives in cataclysmic explosions called supernovae. Massive stars are about ten times heavier and four times larger than our sun, they are also incredibly hot, as their hydrogen burns much more furiously. This means that their fuel is consumed at a much greater rate and runs out after approximately 10 million years, which is relatively short time for a star. Like any other star, massive stars are a balance between heat, which pushes gas up to the surface of the star and gravity, which pulls everything back toward the center. When its core runs out of fuel for fusion, the star can no longer create outward pressure to balance the inward gravitational pull of its great mass. This leads to its dramatic collapse.

The core of the collapsing star shrinks, becoming hotter and denser in the process, as iron atoms are crushed together. During this time the core temperature shoots to about 100 billion degrees. This explosive release of energy results in a huge expanding shock wave and the outer layers of the star are thrown outward at 10^9 kph. This giant explosion is known as a supernova. The material which is exploded away from the star slams into surrounding lumps and clouds of gas. It heats up and begins to glow forming an expanding ring known as a supernova remnant.

All that remains of the original star is a small super dense core composed entirely of neutrons, known as a neutron star. Most of these turn on and radiate. When this happens, a pulsar has been formed. (Interestingly, if the star is greater than 15 times as massive as the sun, then its neutrons cannot survive the collapse of the core due to the increased inward gravitational pull these stars become black

holes).

1.4 Pulsars as Radio Sources

The periodic beacon sent by the pulsar clock is usually rather weak, both because the pulsar is distant and the size of the actual emission region is small. Estimates range down to a few meters, resulting in brightness temperatures of up to 10^{37} K [17]. Such values require a coherent emission mechanism which, despite almost 40 years of intensive research, is still unidentified. However, we seem to have some basic understanding, in which the magnetized rotating neutron star induces an electric quadrupole field which is strong enough to pull out charges from the stellar surface (the electrical force exceeds the gravitational force by a factor of $\sim 10^{12}$), surrounding the pulsar with dense plasma. The magnetic field forces the plasma to co-rotate with the pulsar like a rigid body. This co-rotating magnetosphere can only extend up to a distance where the co-rotation velocity reaches the speed of light [18]. This distance defines the so-called light cylinder which separates the magnetic field lines into two distinct groups, i.e. open and closed field lines. Closed field lines are those which close within the light cylinder, while open field lines would close outside. The plasma on the closed field lines is trapped and will co-rotate with the pulsar forever. In contrast, plasma on the open field lines can reach highly relativistic velocities and can leave the magnetosphere, creating the observed radio beam at a distance of a few tens to hundreds of km above the pulsar surface (see fig 1.1). Most pulsars are not strong enough to allow us a detection of their individual radio pulses, so that in most cases only an integrated pulse shape can be observed. If individual pulses are observable, they reflect the instantaneous plasma processes in the pulsar magnetosphere at the moment when the beam is directed towards Earth. The dynamics of these processes results in often seemingly random individual pulses, in particular when viewed with high time resolution. Despite this variety displayed by the single pulses, the mean pulse shape computed by averaging a few hundreds to few thousands of pulses is incredibly stable [19].

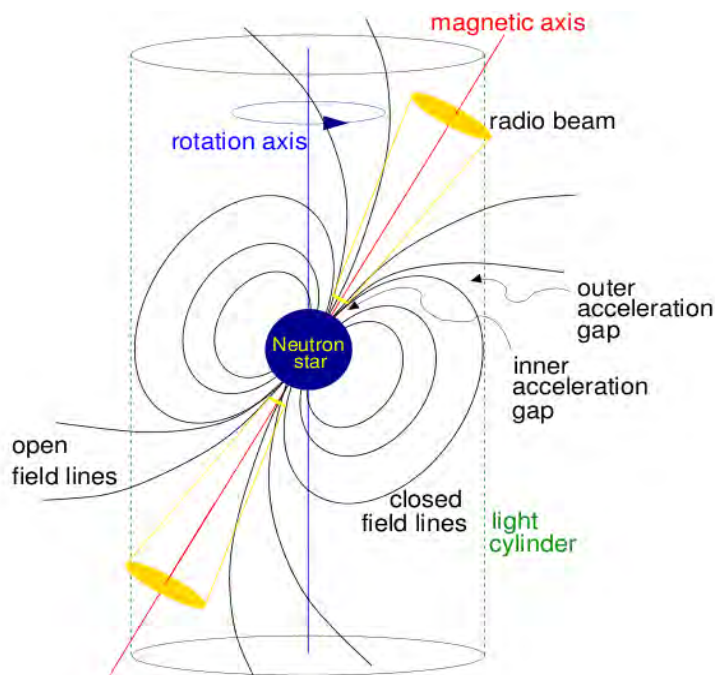


Figure 1.1: A pulsar is a rotating, highly magnetized neutron star. A radio beam centered on the magnetic axis is created in some distance to the pulsar. The tilt between the rotation and magnetic axes makes the pulsar in effect a cosmic light house when the beam sweeps around in space.

In contrast to the snapshot provided by the individual pulses, the average pulse shape, or pulse profile, can be considered as along-exposure picture, revealing the global circumstances in the magnetosphere. These are mostly determined by geometrical factors and the strong magnetic field, leading to very stable pulse profiles. Apart from a distinct evolution with radio frequency, the same profiles are obtained, no matter where and when the pulses used to compute the average have been observed.

Chapter 2

Braking Index Diagnostics

2.1 Braking Index of Pulsar

Neutron stars are powered by rotational kinetic energy and lose energy by emitting electromagnetic radiation at their rotation frequency Ω . The rotation frequency thus decreases with time and this slowdown is usually described by the relation

$$\dot{\Omega} = -\kappa\Omega^n \quad (2.1.1)$$

where, κ is a positive constant which depends on the moment of inertia and the magnetic dipole moment of the neutron star, n is the braking index. Conventionally, the braking index is derived by differentiation of eq.(2.1.1), yielding

$$n = \frac{\Omega\ddot{\Omega}}{\dot{\Omega}^2} \quad (2.1.2)$$

In a highly simplified model in which the spin down torque arises from dipole radiation at the rotation frequency, one expects $n = 3$.

Only 4 pulsars have had their braking indices measured and all have $n < 3$. The Crab pulsar has a value 2.509 ± 0.01 (Lyne, Pritchard & Smith 1988; Lyne, Pritchard & Smith 1993)[20], *PSR1509 – 58* has a braking index 2.837 ± 0.02 (Kaspi et al. 1994), *PSR0540 – 69* has $n = 2.04 \pm 0.02$ (Manchester & Peterson 1989[21]; Nagase et al.1990[22]; Gouiffes, Finley & ogelman 1992 [23]) and, finally, the Vela pulsar has the low value 1.4 ± 0.2 (Lyne et al. 1996).(Melatos 1997) has shown that a modification of the simple model, which involves treating the neutron star and the inner magnetosphere as one entity, allowed him to derive

values of braking index very close to those observed (except for the Vela pulsar). Braking indices are very difficult to measure in all the other pulsars. For a typical 'old' pulsar with $\Omega = 1Hz$, $\dot{\Omega} = 10^{-15}Hzs^{-1}$, the expected $\ddot{\Omega}$ from eq.(2.1.2) is only $\sim 10^{-30}Hzs^{-2}$, much too small to measure even over hundreds of years of timing the second derivative only contributes one extra phase rotation every 600 year! There are a number of pulsars with ages ~ 20 kyr for which one might expect to be able to measure n . However, two different effects tend to dominate the value of $\ddot{\Omega}$ over that expected from spin-down alone. First, these young pulsars glitch often (Shemar & Lyne 1996)[24]. These glitches lead to discontinuities in both Ω and $\dot{\Omega}$ making it very difficult to phase connect i.e. count the exact number of rotations of the pulsar over the glitch. Furthermore, the recovery from a glitch can last many hundreds of days and the measurement of $\dot{\Omega}$ reflects the recovery rather than the intrinsic spin-down. Finally, young pulsars have large random variations in arrival times known as 'timing noise'. (Cordes & Helfand 1980)[25] recognised that the timing noise dominates over the intrinsic $\ddot{\Omega}$ by a factor ~ 100 in these pulsars and that many early published values of braking indices, based on $\ddot{\Omega}$ were spurious.

Instead of differentiating eq.(2.1.1), we integrate from a time t to $t + T$ to obtain

$$\frac{\dot{\Omega}}{\Omega^n} = -\kappa \quad (2.1.3)$$

$$\int_{\Omega_1}^{\Omega_2} \frac{\dot{\Omega}}{\Omega^n} d\Omega = - \int_t^{t+T} \kappa dt \quad (2.1.4)$$

$$\frac{\Omega_2^{(1-n)} - \Omega_1^{(1-n)}}{1-n} = -\kappa(T + t - t) \quad (2.1.5)$$

from eq.(2.1.3) substitut the value of κ in to eq.(2.1.5) which follows

$$\frac{\Omega_2^{(1-n)} - \Omega_1^{(1-n)}}{1-n} = \frac{\dot{\Omega}_1 T}{\Omega_1^n} \quad (2.1.6)$$

Hence

$$1 - n = \frac{(\Omega_2^{1-n} - \Omega_1^{1-n})\Omega_1^n}{\dot{\Omega}_1 T} \quad (2.1.7)$$

$$1 - n = \frac{\Omega_2 \left(\frac{\Omega_1}{\Omega_2}\right)^n - \Omega_1}{\dot{\Omega}_1 T} \quad (2.1.8)$$

But $\left(\frac{\Omega_1}{\Omega_2}\right)^n = \frac{\dot{\Omega}_1}{\dot{\Omega}_2}$

$$1 - n = \frac{\Omega_2 \frac{\dot{\Omega}_1}{\dot{\Omega}_2} - \Omega_1}{\dot{\Omega}_1 T} \quad (2.1.9)$$

$$n = 1 + \frac{\Omega_2 \frac{\dot{\Omega}_1}{\dot{\Omega}_2} - \Omega_1}{\dot{\Omega}_1 T} \quad (2.1.10)$$

$$n = 1 + \frac{\dot{\Omega}_2 \Omega_1 - \dot{\Omega}_1 \Omega_2}{\dot{\Omega}_1 \dot{\Omega}_2 T} \quad (2.1.11)$$

This allows the braking index to be computed without the need to measure $\ddot{\Omega}$. The advantage of this method is that, in principle, Ω and $\dot{\Omega}$ can be measured over a short interval of time and then re-measured 20 year later without the need for a phase connected solution over the whole 20 year time span.

2.2 Alignment and Counteralignment

The braking index of a pulsar slowing down via magnetic dipole radiation can be Written (Macy 1974)[3] as

$$n = 3 - \frac{25I_o R \Omega^2}{2GM^2} - \tau \left[\frac{d}{dt} \ln \sin^2 \alpha - \frac{2}{\tau_B} \right] \quad (2.2.1)$$

$$= 3 - \tau \left[2 \cot \alpha \dot{\alpha} - \frac{2}{\tau_B} \right] \quad (2.2.2)$$

Here I_o and R are respectively the moment of inertia and radius of the (rotationally) undistorted star, M is the stellar mass, Ω is the angular frequency, α is the angle between the rotation and magnetic axes and τ_B is the time scale

for magnetic field decay. The first term on the right hand side of Eq.(2.2.1) is that given by the standard model: a perfect sphere with constant magnetic field inclined at a constant angle to the rotation axis. The second term comes from rotational distortion, the effects of which are discussed in detail in (Cowsik, Ghosh & Melvin 1983)[26]. The first part of the third term describes the effects of alignment or counter alignment, and the second part those of magnetic-field decay. Rotational distortion and counter alignment decrease n from its standard value, while field decay and alignment increase it above this value. Since n has been accurately measured only for pulsars with period $p \geq 33$ ms (indeed, $p \sim 1$ s for most of the sample), the effects of rotational distortion are negligible for this sample (Cowsik, Ghosh and Melvin 1983), and we shall neglect these effects in what follows.

For alignment, we adopt Jones model, which gives

$$\alpha(t) = \alpha_o \exp\left(-\frac{t}{\tau_a}\right) \quad (2.2.3)$$

$$\dot{\alpha}(t) = -\frac{\alpha(t)}{\tau_a} \quad (2.2.4)$$

τ_a being the alignment time scale. This gives

$$n_a = 3 - \tau \left[2 \cot \alpha \left(-\frac{\alpha}{\tau_a} \right) - \frac{2}{\tau_B} \right] \quad (2.2.5)$$

$$n = 3 + 2\tau \left[\left(\frac{\alpha}{\tau_a} \right) \cot \alpha + \frac{1}{\tau_B} \right] \quad (2.2.6)$$

For counter alignment, we adopt the form (Flowers & Ruderman 1977[27]; Nowakowski 1983b)

$$\alpha(t) = \frac{\pi}{2} - \left(\frac{\pi}{2} - \alpha_o \right) \exp\left(-\frac{t}{\tau_c}\right) \quad (2.2.7)$$

$$\dot{\alpha}(t) = \frac{1}{\tau_c} \left[\left(\frac{\pi}{2} - \alpha_o \right) \exp\left(-\frac{t}{\tau_c}\right) \right] \quad (2.2.8)$$

τ_c being the counter alignment time scale. This gives (Nowakowski 1983b)[28]

$$n_c = 3 - 2\tau \left[\cot \alpha \frac{1}{\tau_c} \left(\frac{\pi}{2} - \alpha_o \right) \exp\left(-\frac{t}{\tau_c}\right) - \frac{1}{\tau_B} \right] \quad (2.2.9)$$

$$= 3 + 2\tau \left[\frac{1}{\tau_B} - \frac{1}{\tau_c} \left(\frac{\pi}{2} - \alpha_o \right) \exp\left(-\frac{t}{\tau_c}\right) \cot\left(\frac{\pi}{2} - \left(\frac{\pi}{2} - \alpha_o \right) \exp\left(-\frac{t}{\tau_c}\right)\right) \right] \quad (2.2.10)$$

$$= 3 + 2\tau \left[\frac{1}{\tau_B} - \frac{1}{\tau_c} \left(\frac{\pi}{2} - \alpha_o \right) \exp\left(-\frac{t}{\tau_c}\right) \frac{\cos\left(\frac{\pi}{2} - \left(\frac{\pi}{2} - \alpha_o \right) \exp\left(-\frac{t}{\tau_c}\right)\right)}{\sin\left(\frac{\pi}{2} - \left(\frac{\pi}{2} - \alpha_o \right) \exp\left(-\frac{t}{\tau_c}\right)\right)} \right] \quad (2.2.11)$$

$$= 3 + 2\tau \left[\frac{1}{\tau_B} - \frac{1}{\tau_c} \left(\frac{\pi}{2} - \alpha_o \right) \exp\left(-\frac{t}{\tau_c}\right) \tan\left(\frac{\pi}{2} - \alpha_o \right) \exp\left(-\frac{t}{\tau_c}\right) \right] \quad (2.2.12)$$

The variations of n_a and n_c with τ are shown in Fig 2.1. We have chosen various values of τ_B in the range $10^6 - 10^7$ years, in agreement with current understanding of the magnetic-field decay processes, and have tried various values of τ_a and τ_c in the range $10^3 - 10^7$ years. We see that, due to alignment and field decay (particularly alignment), n can become orders of magnitude larger than its standard value of 3 and thus explains the observed large positive values of n and so the large negative values of \ddot{p} , (Gullahorn & Rankin 1982)[29]; (Manchester et al. 1983)[30];(Nowakowski 1983(a, b))[31]. Counter alignment does reduce n below its standard value (and can make $\ddot{p} > 0$, but does not lead to negative values of n . The counter alignment curves shown in Fig. 2.1 correspond to $\alpha_0 = 0$ (alignment at $t = 0$), which maximizes the counter alignment effects. At large τ , the field-decay effects dominate, and the counter alignment curves also rise to large positive values of n . For the alignment curves shown in Fig.2.1, different values of τ_B in the $10^6 - 10^7$ year range make no visible difference. Similarly, for the counter alignment curves shown, different values of τ_c in the $10^3 - 10^7$ year

range make little visible difference. Hence, the former curves are labeled by values of τ_a and the latter by those of τ_B . The data on 19 pulsars for which $\ddot{\Omega}$ has been measured are shown in Fig.2.1 (Gullahorn & Rankin 1978a, 1982; Demiaski & Prszyski 1979[32] and the references therein; Downs 1981[33]) and displayed in Table 1. We have not included those pulsars for which only an upper limit to $\ddot{\Omega}$ is available. The data fall into two distinct classes, eleven pulsars with $n >$ and eight with $n < 0$ (Table 1).

Psr	Ω (Hz)	$\dot{\Omega}$ (Hz s ⁻¹)	$\ddot{\Omega}$ (Hz s ⁻²)	braking index $n = \frac{\dot{\Omega}\Omega}{\ddot{\Omega}}$	slowing down age τ (yr)
0329 +54[32]	1.4	-4.02E - 15	...	(4.81 ± 0.18)E ₃	1.11E ₇
0531 +21[44]	30.18	-3.848E - 10	(1.234 ± 0.002)E - 20	(2.515 ± 0.005)E ₀	2.49E ₃
0540 +23[29]	4.066	-2.550E - 13	(3.953 ± 0.082)E - 25	(2.5 ± 0.05)E ₁	5.16E ₅
0611 +22[25]	2.986	-5.31E - 13	...	(3.5)E ₂	1.78E ₅
0823 +26[25]	1.884	-6.06E - 15	...	(-1)E ₄	9.87E ₆
0833 -45[33]	11.21	-1.57E - 11	(9.2 ± 2.61)E - 22	(4.2 ± 13)E ₁	2.27E ₄
0950 +08[29]	3.951	-3.578E - 15	(-1.704 ± 0.124)E - 25	(-5.2 ± 0.4)E ₄	3.47E ₇
1508+ 55[35]	1.352	-9.20E - 15	...	(3.25)E ₃	4.66E ₆
1541 +09[29]	1.336	-7.682E - 16	(-1.116 ± 0.091)E - 25	(-2.5 ± 0.2)E ₅	5.52E ₇
1604 -00[29]	2.371	-1.720E - 15	(2.310 ± 0.448)E - 26	(1.8 ± 0.4)E ₄	4.38E ₇
1859 +03[29]	1.526	-1.743E - 14	(1.100 ± 0.050)E - 24	(5.5 ± 0.05)E ₃	2.78E ₆
1900 +01[29]	1.371	-7.58E - 15	(2.1 ± 0.5)E - 25	(5.0 ± 1.2)E ₃	5.74E ₆
1907 +00[29]	0.983	-1.13E - 14	(-2.5 ± 0.2)E - 25	(-8.7 ± 0.7)E ₃	5.85E ₆
1907 +02[29]	2.021	3.277E - 15	(-6.0 ± 2.0)E - 26	(-9.5 ± 3.1)E ₂	5.68E ₆
1907 +10[29]	3.526	3.27E - 14	(-1.689 ± 0.06)E - 24	(-5.5 ± 0.2)E ₃	3.42E ₆
1915 +13[29]	5.138	1.30E - 14	(-6.440 ± 0.505)E - 25	(-4.2 ± 0.3)E ₁	8.58E ₅
1929 +10[29]	4.415	0.38E - 14	(-3.180 ± 0.150)E - 25	(-2.8 ± 0.1)E ₃	6.23E ₆
2002 +31[29]	0.4737	1.39E - 14	(7.126 ± 0.268)E - 26	(1.2 ± 0.05)E ₂	8.99E ₅
2020 +28[29]	2.912	0.51E - 14	(1.028 ± 0.080)E - 25	(1.2 ± 0.1)E ₃	5.75E ₆

Table 1:Braking index.

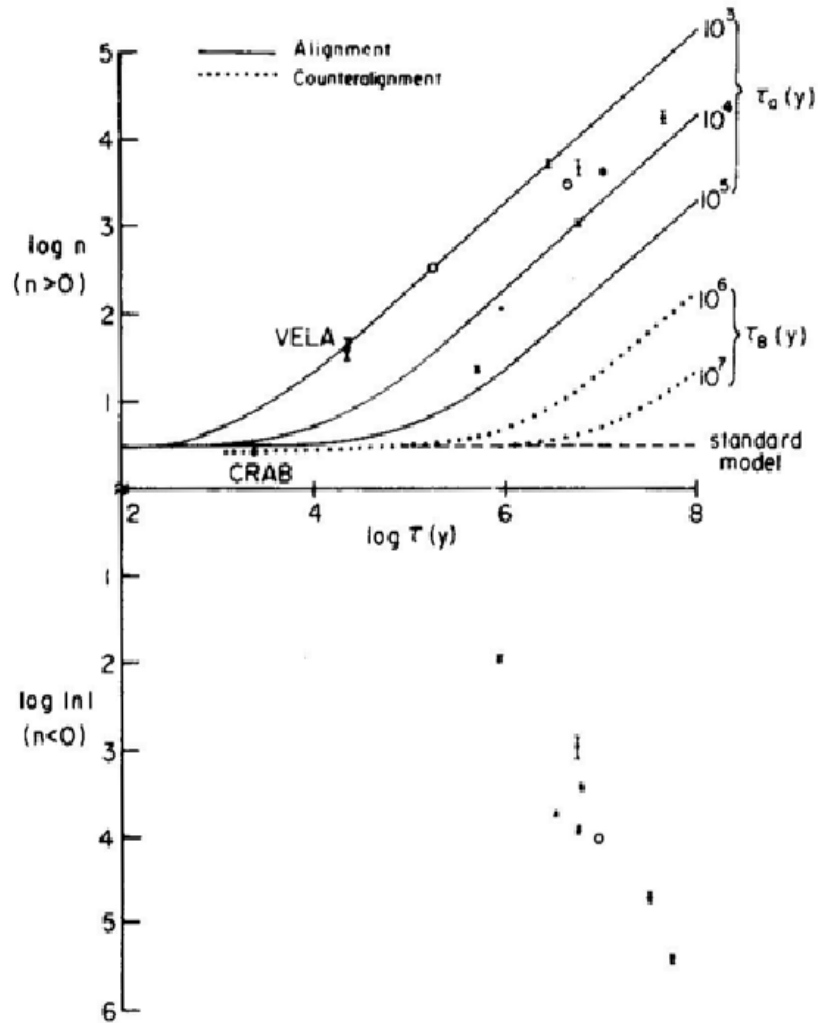


Figure 2.1: Braking Index Vs slowing-down-Age Correlation. Plotted is the logarithm of the absolute value of the braking index against the logarithm of age. Also shown are the theoretical curves for alignment (solid lines), those for counteralignment (dotted lines) and that given by the Standard $n = 3$ model (dashed line). The alignment curves are labelled by alignment timescales, τ_a ; different values of the field decay timescale, τ_B , in the range $(10^6 - 10^7)$ year make no visible difference for these curves. The counteralignment curves are labelled by τ_B , different values of the counteralignment timescale, τ_c , in the range $(10^3 - 10^7)$ year make little visible difference for these curves. Filled circles: measurements quoted with error bars as shown. Open circles: measurements quoted without error bars.

In each class, there is a strong correlation (indeed an almost obvious linear relation) between $\log |n|$ and $\log \tau$.

The theoretical curves for alignment are consistent with the $n > 0$ data for $\tau_a \sim 10^3 - 10^5$ year (the effect on these curves of varying τ_B in the range $10^6 - 10^7$ year is negligible). The curves for counter alignment are inconsistent with the $n > 0$ data. (The case of Crab pulsar, which has $n \simeq 2.5$, is a special one, and is discussed later). The $n < 0$ data are in complete disagreement with either alignment or counter alignment. It is thus clear from the braking index data available at the present time that there is no evidence for general counter alignment in pulsars. This is in contradiction with the conclusion of Nowakowski (1983b), who did not attempt a quantitative comparison of theory with observation.

2.3 Slowing-down noise

The secular nature of the apparent second derivatives of pulsar periods has been questioned before (Cordes & Helfand 1980 and references therein). The facts that almost half the known sample shows unexplained large negative braking indices, and that both halves show essentially the same strong correlation between the absolute value of the braking index and the slowing-down age, make us reconsider this point. Random walks in phase, frequency, or the first derivative of frequency can give rise to apparent second derivatives. For the last case, that of the so-called slowing-down noise, the apparent second derivative, $\langle \ddot{\Omega}_R \rangle$, is related to the rms residual, $\sigma_R(2, T)$, of a least squares second-order polynomial fit to the timing data over an interval of length T through the inequality (Cordes & Helfand 1980)

$$\langle \ddot{\Omega}_R \rangle \lesssim \frac{120\sqrt{7}}{T^3 p} \sigma_R(2, T) \quad (2.3.1)$$

This immediately gives

$$|n_R| \leq \left(\frac{\tau}{\tau_R}\right)^2 \quad (2.3.2)$$

where

$$\tau_R = \left(\frac{120\sqrt{7}\sigma_R(2, T)}{T^3} \right)^{-1/2} \quad (2.3.3)$$

is the random-noise age τ_R is determined by the nature of the noise processes and by the observation interval . $\sigma_R(2, T)$ and T have been given by (Cordes & Helfand 1980) for 16 of the 19 pulsars considered here. In Table 2, we give the values of τ_R and $\langle |nR| \rangle$, and compare $\langle |nR| \rangle$ with the observed $\langle |n| \rangle$ in Fig. 2.2 and Table 2. For all but the Crab and Vela pulsars, there is excellent agreement, $|n|_{obs}$ always lying below the upper limit on $\langle |nR| \rangle$ given by Eq.(2.3.2) with two slight exceptions. For Crab and Vela, $\langle |nR| \rangle_{max}$ are far below the observed values. We thus arrive at the conclusion that for aging pulsars ($\tau \geq 10^5$ year) which show apparent braking indices whose magnitudes are very much larger than 3, the second derivative may very well be dominated by slowing down noise, whereas for the young Crab and Vela pulsars, the second derivative cannot be so dominated.

psr	T(d)	$\sigma_R(2, T)$ (ms)	τ_R (yr)	$\langle nR \rangle$	observed
0329 +54	2859	2.31	$1.44E_5$	$5.95E_3$	$(4.81 \pm 0.18)E_3$
0531 +21	1628	11.97	$2.72E_4$	$8.4E_3$	$(2.515 \pm 0.005)E_0$
0540 +23	1368	0.52	$1.00E_5$	$2.64E_1$	$2.5 \pm 0.05E_1$
0611 +22	1586	107.00	$8.74E_3$	$4.15E_2$	$(3.5)E_2$
0823 +26	1834	12.55	$3.17E_4$	$9.68E_4$	$(1)E_4$
0833 -45	1000	4.2 -32.0	$2.21E_4$	$1.06 - 8.05E_0$	$(4.2 \pm 2.3)E_1$
0950 +08	1563	0.45	$1.32E_5$	$6.93E_4$	$(5.2 \pm 0.4)E_4$
1508+55	2865	5.67	$9.21E_4$	$2.56E_3$	$(3.25)E_3$
1541 +09	1669	0.95	$1.00E_5$	$3.04E_5$	$(2.5 \pm 0.2)E_5$
1604 -00	2134	0.33	$2.53E_5$	$3.00E_4$	$(1.8 \pm 0.4)E_4$
1859 +03	1227	3.98	$3.08E_4$	$8.13E_3$	$(5.5 \pm 0.05)E_3$
1907 +10	1107	1.40	$4.45E_4$	$5.9E_3$	$(5.5 \pm 0.2)E_3$
1915 +13	1603	1.30	$8.05E_4$	$1.13E_2$	$(4.2 \pm 0.3)E_1$
1929 +10	1334	0.38	$1.13E_5$	$3.03E_3$	$(2.8 \pm 0.1)E_3$
2002 +31	1607	1.39	$7.82E_4$	$1.32E_2$	$(1.2 \pm 0.05)E_2$
2020 +28	2047	0.51	$1.86E_5$	$9.6E_2$	$(1.2 \pm 0.1)E_2$

Table 2: slowing down noise.

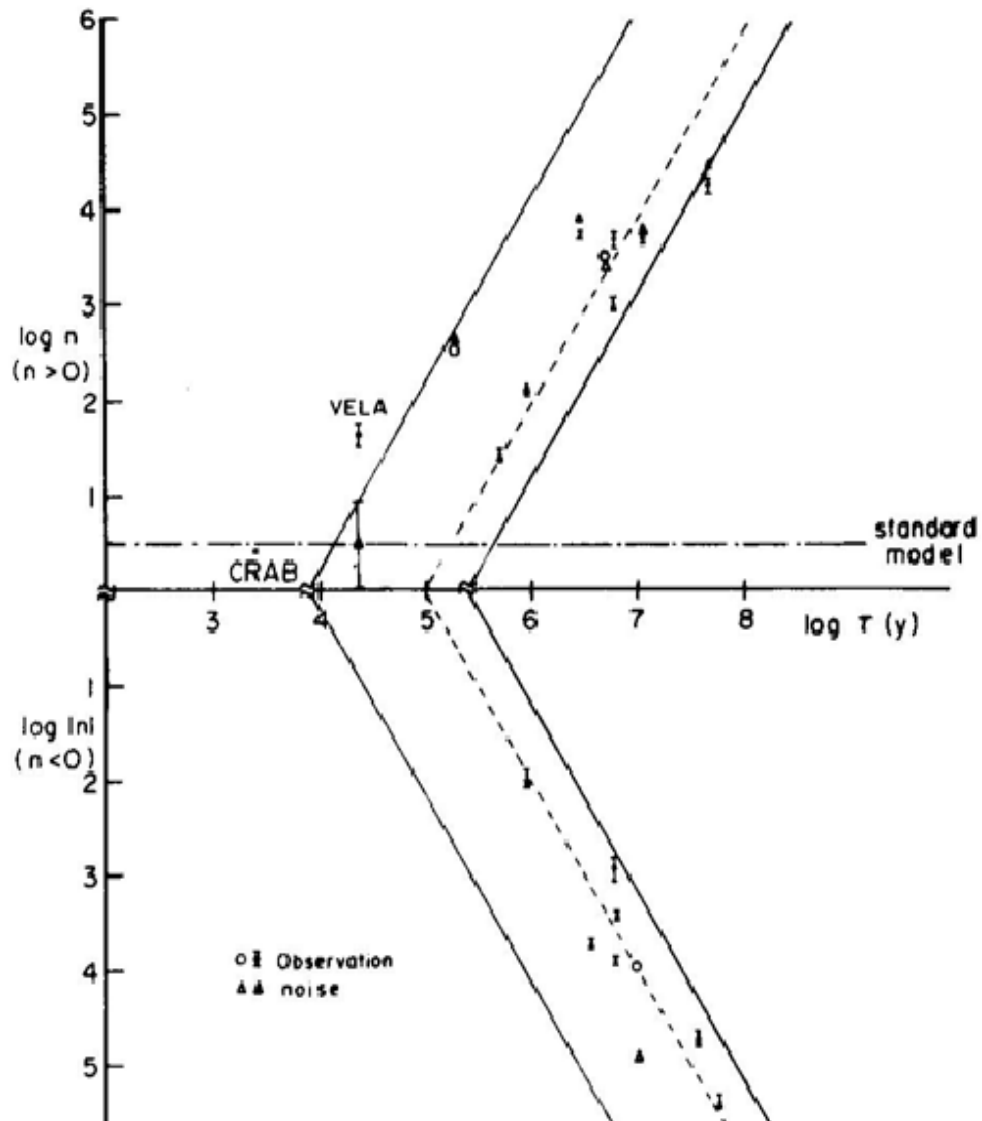


Figure 2.2: Same as Fig. 2.1, but comparing the observed braking indices (circles) with those expected from slowing-down noise (triangles). Filled circles: measurements quoted with error bars as shown. open circles: measurements quoted without error bars. For vela, the slowing down noise component itself has an uncertainty as shown (Downs 1981). Also shown are the noise-band (the area between the two solid lines which corresponding to the maximum and minimum values of τ_R in Table 2) and the relation $|n| - (\frac{\tau}{10^5 \text{ year}})^2$ (dashed line) which describes most pulsars adequately.

Chapter 3

Braking Mechanisms of Pulsars

3.1 Electromagnetic Radiation

As it is well known, the electromagnetic torque implies an evolution of the pulsar rotation frequency given by the relation

$$\dot{\Omega}_{em} = -\kappa_{em}\Omega^{n_{em}} \quad (3.1.1)$$

The electromagnetic index is $n_{em} = 3$ for pure dipolar magnetic radiation (Ostriker & Gunn 1969 [34]; Manchester & Taylor 1977 [35]), in which case

$$\kappa_{em} = \frac{2B^2R^6}{3c^3I} \sin^2 \alpha \quad (3.1.2)$$

In this equation B is the strength of the magnetic field, R is the neutron star radius, α is the angle between the rotation and the magnetic axes, and I is the moment of inertia with respect to the rotation axis. An electromagnetic braking index different from 3 can be the consequence of pulsar winds, in which particles having angular momentum are accelerated away from the pulsar (Goldreich & Julian 1969[36];Kaspi et al. 1994) or can be produced if non dipolar components of the magnetic field are present, or as a consequence of strong magnetospheric currents (Blandford & Romani 1988)[38]. Another possibility is that the magnetic moment, and then the torque applied to the star, varies in time (Blandford & Romani 1988; Cheng 1989[39]). (Muslimov & Page 1996)[40] consider the time evolution of the surface magnetic field of the star, which according to their model, is very low ($10^8 \div 10^9 G$) for a new born neutron star and then increases due to the ohmic diffusion of the initially trapped inner magnetic field. The resulting electromagnetic

braking index is given by

$$n_{em} = 3 + 2 \frac{\dot{B}_{surf} \Omega}{B_{surf} \dot{\Omega}} \quad (3.1.3)$$

where B_{surf} is the value of the surface magnetic field at the magnetic pole. Clearly, if $\dot{B}_{surf} > 0$, $n_{em} < 3$. Other models based on the secular variation of the magnetic field have been developed, for instance, by (Blandford et al. 1983)[41] and by (Camilo 1996)[42]. A different kind of model has been proposed by (Allen & Horvath 1997) and by (Link & Epstein 1997)[43], based on the growth of the angle α between the magnetic moment and the rotation axis of the star. In this case the electromagnetic braking index is

$$n_{em} = 3 + 2 \frac{\dot{\alpha} \Omega}{\tan \alpha \dot{\Omega}} \quad (3.1.4)$$

In all these cases the general expression for the observed electromagnetic braking index is simply

$$n_{em} = 3 + \frac{\dot{\kappa}_{em} \Omega}{\kappa_{em} \dot{\Omega}_{em}} \quad (3.1.5)$$

which is easily obtained differentiating Eq.(3.1.1) with respect to time. From Eq.(3.1.2) we find

$$\frac{\dot{\kappa}_{em}}{\kappa_{em}} = \frac{2\dot{B} \sin^2 \alpha + B \sin 2\alpha \dot{\alpha} - B \sin^2 \alpha \frac{\dot{I}}{I}}{B \sin^2 \alpha} \quad (3.1.6)$$

$$= 2 \frac{\dot{B}}{B} + 2 \frac{\cos \alpha}{\sin \alpha} \dot{\alpha} - \frac{\dot{I}}{I} \quad (3.1.7)$$

$$= 2 \frac{\dot{B}}{B} + 2 \cot \alpha \dot{\alpha} - \frac{\dot{I}}{I} \quad (3.1.8)$$

Assuming $n_{em} = \text{constant}$, from Eq.(3.1.5) we find

$$\kappa_{em} = \kappa_{em,0} \times \left(\frac{\Omega}{\Omega_o} \right)^{n_{em}-3} \quad (3.1.9)$$

where $\kappa_{em,0}$ and Ω_o are the electromagnetic torque function and the angular velocity at time $t = 0$, i.e now. Then, the rate of variation of the angular velocity can be written as

$$\dot{\Omega}_{em} = \kappa_{em,eff} \times \Omega^{n_{em}} \quad (3.1.10)$$

where $\kappa_{(em,eff)} = \frac{\kappa_{(em,0)}}{\Omega_o^{n_{em}-3}}$ is a constant, which is formally equivalent to Eq.(3.1.1). Integrating Eq.(3.1.1) we obtain the pulsar characteristic time, due to the electromagnetic braking which is

$$\tau_{em} = \frac{\Omega_o}{(1 - n_{em})\dot{\Omega}_o} \left[1 - \left(\frac{\Omega_o}{\Omega_i} \right)^{n_{em}-1} \right] \quad (3.1.11)$$

Ω_i being the initial angular velocity of the pulsar. Eq.(3.1.11) would give the true age if only the electromagnetic emission was responsible for the pulsar spin-down. From Eq.(3.1.1, 3.1.2) and from rotation energy loss the strength of the magnetic field, for $n_{em} = 3$, is

$$\dot{E}_{rot} = I\dot{\Omega}_{em}\Omega_{em} = \frac{2B^2 R^6 \sin^2 \alpha \Omega_{em}^4}{3c^3} \quad (3.1.12)$$

$$B^2 = \frac{3c^3 I \dot{\Omega}_{em}}{2R^6 \sin^2 \alpha \Omega_{em}^3} \quad (3.1.13)$$

The angular velocity of rotation of the neutron star $\Omega_{em} = \frac{2\pi}{p}$, can be used, these being related by

$$\frac{\dot{\Omega}_{em}}{\Omega_{em}} = \frac{\dot{p}_{em}}{p_{em}} \quad (3.1.14)$$

$$B \sin \alpha = \sqrt{\frac{3c^3 I \dot{\Omega}_{em}}{2R^6 \Omega_{em}^3}} \quad (3.1.15)$$

$$B \sin \alpha = \sqrt{\frac{3c^3 I \dot{p}_{em} p_{em}}{8\pi^2 R^6}} \quad (3.1.16)$$

$$B \sin \alpha = 3.2 \times 10^{19} \sqrt{\dot{p}_{em} p_{em}} \quad (3.1.17)$$

where α is the angle between the magnetic and the rotation axis, \dot{p}_{em} is the rate of variation of the pulsar period due to the electromagnetic torque, and we have assumed $I \simeq 10^{38} \text{kgm}^2$.

3.2 Electromagnetic plus Gravitational Radiation

In this section we show that the observed braking indexes can result from the combined action, in a pulsar, of the magnetic and gravitational torques. We assume that the emission of electromagnetic and gravitational radiation are the only mechanisms acting on the pulsar. The observed spin-down rate can be expressed as

$$\dot{\Omega} = - \sum_{\alpha} \kappa_{\alpha} \Omega^{n_{\alpha}} = \dot{\Omega}_{em} + \dot{\Omega}_{gw} \quad (3.2.1)$$

where α stands for em and gw processes respectively

$$\ddot{\Omega} = - \sum_{\alpha} \dot{\kappa}_{\alpha} \Omega^{<n_{\alpha}>} - \sum_{\alpha} \kappa_{\alpha} <n_{\alpha}> \Omega^{<n_{\alpha}>-1} \dot{\Omega} \quad (3.2.2)$$

$$\ddot{\Omega}\Omega = - \sum_{\alpha} \dot{\kappa}_{\alpha} \Omega^{<n_{\alpha}>} \Omega - \sum_{\alpha} \kappa_{\alpha} <n_{\alpha}> \Omega^{<n_{\alpha}>-1} \dot{\Omega}\Omega \quad (3.2.3)$$

$$\ddot{\Omega}\Omega = - \sum_{\alpha} \dot{\kappa}_{\alpha} \Omega^{<n_{\alpha}>+1} - \sum_{\alpha} \kappa_{\alpha} <n_{\alpha}> \Omega^{<n_{\alpha}>} \dot{\Omega} \quad (3.2.4)$$

$$\dot{\Omega}^2 = - \dot{\Omega} \sum_{\alpha} \kappa_{\alpha} \Omega^{<n_{\alpha}>} \quad (3.2.5)$$

$$\frac{\ddot{\Omega}\Omega}{\dot{\Omega}^2} = \frac{- \sum_{\alpha} \dot{\kappa}_{\alpha} \Omega^{<n_{\alpha}>+1} - \sum_{\alpha} \kappa_{\alpha} <n_{\alpha}> \Omega^{<n_{\alpha}>} \dot{\Omega}}{- \dot{\Omega} \sum_{\alpha} \kappa_{\alpha} \Omega^{<n_{\alpha}>}} \quad (3.2.6)$$

$$\frac{\ddot{\Omega}\Omega}{\dot{\Omega}^2} = \frac{\sum_{\alpha} \dot{\kappa}_{\alpha} \Omega^{<n_{\alpha}>+1}}{\sum_{\alpha} \kappa_{\alpha} \Omega^{<n_{\alpha}>} \dot{\Omega}} + \frac{\sum_{\alpha} \kappa_{\alpha} <n_{\alpha}> \Omega^{<n_{\alpha}>} \dot{\Omega}}{\sum_{\alpha} \kappa_{\alpha} \Omega^{<n_{\alpha}>} \dot{\Omega}} \quad (3.2.7)$$

$$\frac{\ddot{\Omega}\Omega}{\dot{\Omega}^2} = \frac{\dot{\kappa}_{em}\Omega^{\langle n_{em} \rangle + 1} + \dot{\kappa}_{gw}\Omega^{\langle n_{gw} \rangle + 1}}{(\kappa_{em}\Omega^{\langle n_{em} \rangle} + \kappa_{gw}\Omega^{\langle n_{gw} \rangle})\dot{\Omega}}$$

$$+ \frac{\kappa_{em}\langle n_{em} \rangle\Omega^{\langle n_{em} \rangle} + \kappa_{gw}\langle n_{gw} \rangle\Omega^{\langle n_{gw} \rangle}}{\kappa_{em}\Omega^{\langle n_{em} \rangle} + \kappa_{gw}\Omega^{\langle n_{gw} \rangle}} \quad (3.2.8)$$

we expected as $\kappa_{em}\Omega^{\langle n_{em} \rangle} \gg \kappa_{gw}\Omega^{\langle n_{gw} \rangle}$ for $\tau > 10^3$ years

$$\frac{\ddot{\Omega}\Omega}{\dot{\Omega}^2} = \frac{\dot{\kappa}_{em}\Omega}{\kappa_{em}\dot{\Omega}} \left[\frac{\Omega^{\langle n_{em} \rangle} + \frac{\dot{\kappa}_{gw}\Omega^{\langle n_{gw} \rangle}}{\dot{\kappa}_{em}}}{\Omega^{\langle n_{em} \rangle} + \frac{\kappa_{gw}\Omega^{\langle n_{gw} \rangle}}{\kappa_{em}}} \right]$$

$$+ \frac{\kappa_{em}\Omega^{\langle n_{em} \rangle}}{\kappa_{em}\Omega^{\langle n_{em} \rangle}} \left[\frac{\langle n_{em} \rangle + \frac{\kappa_{gw}\langle n_{gw} \rangle\Omega^{\langle n_{gw} \rangle}}{\kappa_{em}\Omega^{\langle n_{em} \rangle}}}{1 + \frac{\kappa_{gw}\Omega^{\langle n_{gw} \rangle}}{\kappa_{em}\Omega^{\langle n_{em} \rangle}}} \right] \quad (3.2.9)$$

$$= \langle n_{em} \rangle + \frac{\dot{\kappa}_{em}\Omega^{\langle n_{em} \rangle}}{\kappa_{em}\dot{\Omega}^{\langle n_{em} \rangle}} \left[\frac{1 + \frac{\dot{\kappa}_{gw}\Omega^{\langle n_{gw} \rangle}}{\kappa_{em}\Omega^{\langle n_{em} \rangle}}}{1 + \frac{\kappa_{gw}\Omega^{\langle n_{gw} \rangle}}{\kappa_{em}\Omega^{\langle n_{em} \rangle}}} \right] \quad (3.2.10)$$

$$= \langle n_{em} \rangle + \frac{\kappa_{em}\Omega^{\langle n_{em} \rangle}}{\kappa_{em}\dot{\Omega}^{\langle n_{em} \rangle}} \left[1 + \frac{\dot{\kappa}_{gw}\Omega^{\langle n_{gw} \rangle}}{\dot{\kappa}_{em}\Omega^{\langle n_{em} \rangle}} + \frac{\kappa_{gw}\Omega^{\langle n_{gw} \rangle}}{\kappa_{em}\Omega^{\langle n_{em} \rangle}} - \frac{\dot{\kappa}_{gw}\kappa_{gw}\Omega^{\langle n_{gw} \rangle}\Omega^2}{\dot{\kappa}_{em}\kappa_{em}} \right] \quad (3.2.11)$$

where

$$\langle n_{em} \rangle = \frac{\ddot{\Omega}\Omega}{\dot{\Omega}^2} - \frac{\dot{\kappa}_{em}\Omega}{\kappa_{em}|\dot{\Omega}|} \left[1 - \frac{\kappa_{gw}\Omega^{\langle n_{gw} \rangle}}{\kappa_{em}\Omega^{\langle n_{em} \rangle}} \right] \quad (3.2.12)$$

But,
 $\frac{\ddot{\Omega}\Omega}{\dot{\Omega}^2} = 3$

and

Symmetry of neutrino emission cooling behavior with respect to exchanging proton and neutron superfluidities (kaminker et al. 2004)[45]. The magnetic field at any time based on neutrino emission is

$$B(t) = B(o) [1 + t]^{-\frac{1}{6}}$$

Differentiating with respect to time. We obtain

$$\frac{\dot{\kappa}_{em} \Omega}{\kappa_{em} |\dot{\Omega}|} = \frac{1}{6t} \frac{\Omega}{|\dot{\Omega}|}$$

substitut in to eq.(3.2.12) which follows

$$n_{em} = 3 - \frac{1}{6t} \frac{\Omega}{|\dot{\Omega}|} \left[1 - \frac{\kappa_{gw} \Omega^{<n_{gw}>}}{\kappa_{em} \Omega^{<n_{em}>}} \right] \quad (3.2.13)$$

where $\Omega^{<n_{em}>}$ is given by Eq.(3.1.1) or Eq.(3.1.10), while

$$\dot{\Omega}_{gw} = \frac{32GI^2\Omega^5\epsilon^2}{5C^5} = \kappa_{gw}\Omega^5 \quad (3.2.14)$$

where ϵ is the ellipticity of the pulsar.

For the crab pulsar known current parameters are $\Omega = 186.96s^{-1}$, $\dot{\Omega} = -2.33 \times 10^{-9}s^{-2}$, $I \simeq 10^{38}$, $R = 10\text{km}$, $t = 951$ year and $\epsilon = 1.8 \times 10^{-4}$ magnetic field of the crab pulsar is $B \simeq 4 \times 10^{12}G$. From these, we obtain

$$\kappa_{em} = \frac{2B^2R^6 \sin^2 \alpha}{3c^3I} \quad (3.2.15)$$

$$= 0.395 \times 10^{-14} \quad (3.2.16)$$

and

$$\kappa_{gw} = \frac{32GI\epsilon^2}{5C^5} \quad (3.2.17)$$

$$= 0.569 \times 10^{-21} \quad (3.2.18)$$

then

$$\langle n_{em} \rangle = 3 - \frac{1}{6t} \frac{\Omega}{|\dot{\Omega}|} \left[1 - \frac{\kappa_{gw} \Omega^{\langle n_{gw} \rangle}}{\kappa_{em} \Omega^{\langle n_{em} \rangle}} \right] \quad (3.2.19)$$

$$= 3 - 0.45 + 0.45(0.0050) \quad (3.2.20)$$

$$= 3 - 0.45 + 0.00226 \quad (3.2.21)$$

$$\simeq 2.55 \quad (3.2.22)$$

We note that, in analogy with Eq.(3.1.11), the pulsar characteristic age, due to the gravitational braking, is

$$\tau_{em} = -\frac{\Omega_o}{4\dot{\Omega}_o} \left[1 - \left(\frac{\Omega_o}{\Omega_i} \right)^4 \right] \quad (3.2.23)$$

In the following, we will consider the torque functions κ_{em} and κ_{gw} constant in time. The braking index n can be obtained differentiating Eq.(3.2.1), and using Eq.(3.1.1, 3.2.14):

$$n = \frac{\ddot{\Omega}\Omega}{\dot{\Omega}^2} = \frac{n_{em} + 5Y}{1 + Y} \quad (3.2.24)$$

where we have introduced

$$Y = \frac{\dot{\Omega}_{gw}}{\dot{\Omega}_{em}} = \frac{\kappa_{gw} \Omega^{5-n_{em}}}{\kappa_{em}} \quad (3.2.25)$$

This quantity is the ratio between the gravitational and the electromagnetic contributions to the pulsar spin-down rate and we will see in the next that its present values are always less than 1. Note that, in terms of Ω and its derivative,

$$n_{em} = \frac{\ddot{\Omega}_{em}\Omega}{\dot{\Omega}_{em}\dot{\Omega}} \quad (3.2.26)$$

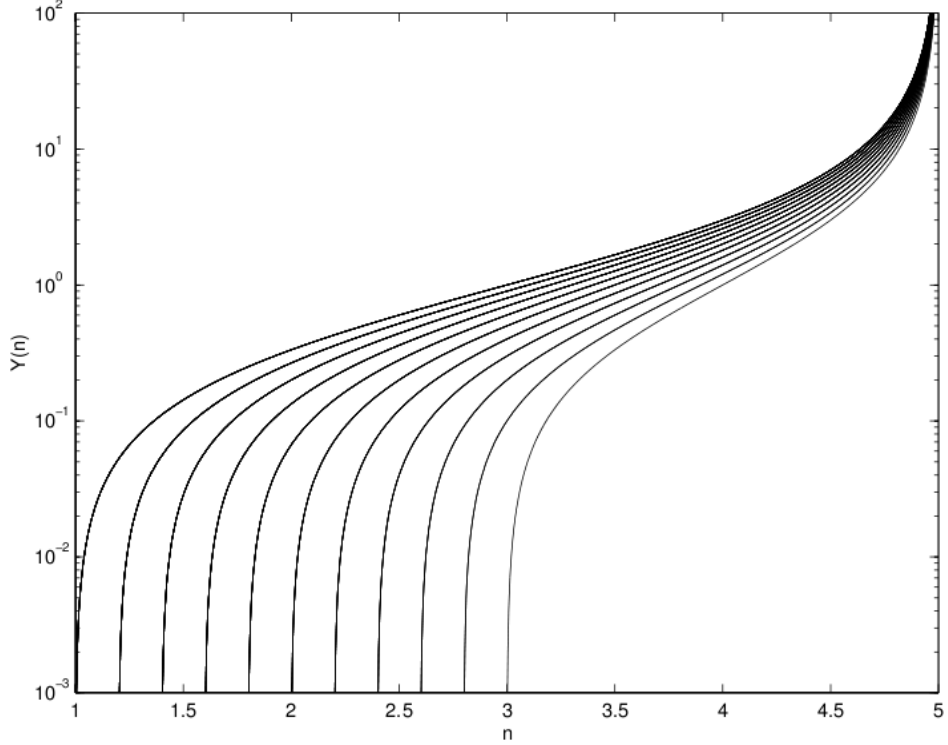


Figure 3.1: $Y(n) = \frac{\dot{\Omega}_{gw}}{\dot{\Omega}_{em}}$ as a function of the braking index n for different values of the electromagnetic braking index n_{em} . n_{em} varies in the range $[1, 3]$ with step 0.2.

Inverting Eq. (3.2.24),

$$Y(n) = \frac{n - n_{em}}{5 - n} \quad (3.2.27)$$

which implies $n_{em} \leq n < 5$. In Fig.3.1 we have plotted the function $Y(n)$ for different values of n_{em} in the range $[1, 3]$: As we expect, for each n_{em} , $Y(n) = 0$ when $n = n_{em}$ (i.e. no gravitational torque) while $Y(n) \rightarrow +\infty$ for $n \rightarrow 5$ (i.e. negligible electromagnetic torque). We see that a braking index less than 3 can be obtained combining the effects of the electromagnetic and gravitational torques. For instance, for the Crab pulsar we have $n = 2.51$ and if we assume, say, $n_{em} = 2.55$, then it immediately follows $Y \simeq 0.016$, that is the gravitational radiation contribution to the spin-down rate is about $\simeq 2$ percent of the electromagnetic one. On the other hand, if $n_{em} = 3$, then $Y \simeq 0.19$. The spin-down of a pulsar in which both the electromagnetic and gravitational torques are acting, Eq.(3.2.1), can be expressed as

$$\dot{\Omega} = \kappa_{eff}(\Omega)\Omega^{n(\Omega)} \quad (3.2.28)$$

where both the effective κ_{eff} and n are function of the angular velocity Ω . As a consequence of its dependence on, the braking index n is not constant in time. From Eq.(3.2.14) we can express the ellipticity of the pulsar as

$$\epsilon = 1.9 \times 10^5 \sqrt{\dot{p}_{gw} p^3} \quad (3.2.29)$$

Combining Eq.(3.2.14, 3.2.25) we can re-write Eq.(3.2.29) as a function of the observed pulsar period and its derivative, and of the ratio Y between the gravitational and electromagnetic spin-down rates:

$$\epsilon = 1.9 \times 10^5 \sqrt{\dot{p} p^3 \frac{Y_{(n)}}{1 + Y_{(n)}}} = 7.55 \times 10^6 \sqrt{\frac{\dot{\Omega}}{\Omega^5} \frac{Y_{(n)}}{1 + Y_{(n)}}} \quad (3.2.30)$$

Equ.(3.2.30) plays a basic role in the determination of the upper limits of the pulsars ellipticity. Then solving for $Y(n)$

$$Y(n) = \frac{A}{1 - A} \quad (3.2.31)$$

where the expression A is equal to

$$A = \frac{\epsilon}{5.70 \times 10^{13}} \frac{\Omega^5}{\dot{\Omega}} \quad (3.2.32)$$

We finally can calculate a lower limit for the electromagnetic braking index n_{em} using eq.(3.2.27)

$$n_{em} = n(1 + Y_n)(5 - n) \quad (3.2.33)$$

3.2.1 Ratio of energy loss due to gravitational versus electromagnetic radiation

Once the spin down limit for a particular pulsar has been reached, we can conclude, that in the absence of a positive detection of gravitational waves, the star is spinning down through a combination of braking mechanisms. For example [21], we can adopt a model that

involve gravitational and electromagnetic braking . In this case the energy loss will be given by

$$\dot{E} = I\Omega\dot{\Omega} = I\Omega[\dot{\Omega}_{em} + \dot{\Omega}_{gw}] \quad (3.2.34)$$

The energy loss due to gravitational waves is given by :

$$\dot{E}_{gw} = I\Omega\dot{\Omega}_{gw} = \frac{32}{5} \frac{G}{c^5} I^2 \epsilon^2 \Omega^6 \quad (3.2.35)$$

while the energy loss due to dipole radiation and other electromagnetic processes is given by

$$\dot{E}_{em} = I\Omega\dot{\Omega}_{em} \quad (3.2.36)$$

Y_n	0.016	upper limit
n_{em}	2.55	lower limit
\dot{E}_{gw} (in percentage)	1.6	upper limit
\dot{E}_{em} (in percentage)	98.4	lower limit

Table 3. upper and lower limits of energy ratio Y_n between gravitational radiation and electromagnetic braking index n_{em} and lower limit of gravitational and electromagnetic radiation contributions \dot{E}_{gw} and \dot{E}_{em} to the total energy loss.

We can also write an expression for the ratio of the contribution of the electromagnetic and gravitational braking to the total energy loss \dot{E}_{tot}

$$\frac{\dot{E}_{em}}{\dot{E}_{tot}} = \frac{1}{(1 + Y_n)} \quad (3.2.37)$$

and

$$\frac{\dot{E}_{gw}}{\dot{E}_{tot}} = \frac{Y_n}{(1 + Y_n)} \quad (3.2.38)$$

Using the crab pulsar observational parameters $n = 2.51$, $\Omega = 186.96s^{-1}$, $\dot{\Omega} = -2.33 \times 10^{-9}s^{-2}$ and latest ellipticity $\epsilon = 1.8 \times 10^{-4}$ from the Lsc(Laser Scientific Collaboration), we obtain current values for the upper and lower limit for the ratio Y_n , the electromagnetic braking index n_{em} and an upper limit on the contribution of gravitational radiation to the total energy loss as illustrated in table 3.

Chapter 4

Discussion and Conclusion

The braking indices of pulsars are different for different pulsars either old or young. Pulsars are powered by rotational kinetic energy and lose energy by emitting electromagnetic radiation at their rotational frequency, Ω . The rotational frequency decreases with time and leads to spin down rate equation and usually described by the eq.(2.1.1). To estimate the contribution alignment and counter alignment of braking indices of pulsars we conclude the following.

- There is no evidence for general counter alignment in the present data on the braking indices of pulsars.
- pulsars with $n > 0$ are consistent with alignment time scales $10^3 - 10^5$ year and field decay on time scales $10^6 - 10^7$ year.
- for all but the crab and vela pulsars, the data can be accounted for by the hypothesis that slowing down noise dominates the measured second derivative of frequency .

In view of the last conclusion do not give consideration to the short alignment time scales found from braking indices ($10^3 - 10^5$ year) . However, it is now clear from eq.(2.2.7) and fig 2.1 .Why short field decay time scales 10^3 year were inferred by Nowkowski(1983 a) on the hypothesis that the large values of n were entirely caused by field decay effects. It is also disturbing to note that short alignment time scales imply a near alignment, and therefor a difficulty in the pulse generation, in the older pulsars. Thus, even for $n > 0$, alignment is not a particularly active mechanism for producing large braking indices .

Braking indices diagnostics can become most useful in studying the basic processes underlying pulsar braking torques when the random noise age τ_R can be made greater than the age of the pulsar (see

eq.2.3.2), since different physical processes will give characteristically different 'tracks' on fig.2.1. Increasing the observation interval T increases τ_R (see eq.2.3.3).

In fact, we can now free the constraint that all the energy loss is due to the emission of gravitational radiation and assume a mixed braking mechanism with contributions from different physical phenomena (gravitational radiation, electromagnetic dipole radiation, winds, magnetosphere currents, fall back disk torques, etc). Different models can be adopted. One of the models we have studied assumes that the electromagnetic braking index is different from the conventional $n = 3$.

In this thesis we show that considering the simultaneous action, in a pulsars of gravitational radiation and electromagnetic one, the observed braking indices can be recovered. The gravitational torque is always a small correlation to the total torque acting on the pulsar. A consequence of the model is that the braking index is not constant in time. We can use the upper limit on the ellipticity to calculate the contribution to the energy loss due to gravitational radiation and calculate the parameter n_{em} , the braking index due to electromagnetic processes. Our current result for the crab pulsar is that the ratio between the energy loss due to gravitational radiation to the energy loss due to electromagnetism is 0.016. This implies that the contribution of the gravitational radiation to the total energy loss has to be less than 2 percent. Finally, the electromagnetic braking index is 2.55 (this is a lower limit).

Alternatively, we can use a model that allows for aclassical electromagnetic dipole but assumes other braking mechanisms to account for a overall braking index different from $n = 3$.

References

- [1] Davis, L., Goldstein, . 1970, *Astrophys. J.*, **159**, L81
- [2] Michel, F. C, Goldwire, H. C. 1970, *Astrophys. Lett.*,**5**, 21
- [3] Macy, W. W. 1974, *Astrophys. J.*, **190**, 153.
- [4] Radhakrishnan, V., Cooke, D. J. 1969, *Astrophys. Lett.*, **3**, 22
- [5] Allen M.P., Horvath J.E., 1997, *MNRAS* **287**, 615
- [6] Lyne A. G., Pritchard R. S., Smith F. G., 1993, *MNRAS*, **265**, 1003
- [7] Boyd P.T., van Citters G.W., Dolan J.F., et al., 1995, *ApJ* **448**, 365
- [8] Kaspi V.M., Manchester R.N., Siegman B., et al., 1994, *ApJ* **422**, L83
- [9] Lyne A. G., Pritchard R. S., Smith F. G., Camilo F., 1996, *Nat*, **381**, 497
- [10] Thorsett, S. E., D. Chakrabarty, *ApJ* **512**, 288 (1999).
- [11] Oppenheimer J. R., Volkoff G., *Phys. Rev.***55**, 374 (1939).
- [12] Zavlin,V. E.,Pavlov, G. G., *A andA* **329**, 583 (1998).
- [13] [http:// www ,atnf,csiro.au /people/pulsar/wwwdev/ Education-page,htm](http://www.atnf.csiro.au/people/pulsar/wwwdev/Education-page.htm).
- [14] Baade.W. and Zwicky F., *Proc. Nat. Acad. Sci.* **20**,254 (1934).
- [15] Pacini, F. (1967), Energy emission from a neutron star, *Nature*, **216**, 567.
- [16] Pranab Ghosh, *Rotation and accretion powered pulsars*. World Scientific, 2007, p.2.

- [17] Hankins, T. H. ,Kern, J. S. , J. C. Weatherall, J. A. Eilek, Nature **422**, 141 (2003).
- [18] Damour, T.,Esposito-Far'se, G., Phys. Rev. D **58**, 1 (1998).
- [19] Blaskiewicz, M. , Ph.D. thesis, Cornell University (1991).
- [20] Lyne A. G., Pritchard R. S., Smith F. G., 1988, MNRAS, 223
- [21] Manchester R. N., Peterson B. A., 1989, ApJ,**342**,L23
- [22] Nagase F., Deeter J., Lewis W., Dotani T., Makino F., Mitsuda K., 1990,ApJ, **351**, L13
- [23] Gouiffes C., Finley J. P., *Ögelman* H., 1992, ApJ,**394**, 581
- [24] Shemar S. L., Lyne A. G., 1996, MNRAS,**282**, 677
- [25] Cordes J. M., Helfand D. J., 1980, ApJ, **239**, 640
- [26] Cowsik, R., Ghosh, P., Melvin, . . 1983, Nature, **303**, 308.
- [27] Flowers, ., Ruderman, . . 1977, Astrophys. J.,**215**, 302.
- [28] Nowakowski, L. A. 1983b, Astr. Astrophys., **127**, 259.
- [29] Gullahorn G. E., Rankin J. M., 1982, ApJ,**260**, 520
- [30] Manchester, R. N., Taylor, J. . 1981, Astrophys. J., **86**, 1953.
- [31] Nowakowski, L. A. 1983a, Astr. Astrophys.,**118**, 29.
- [32] Demiaski, ., Przyski, . 1979, Nature,**282**, 383.
- [33] Downs, G. S. 1981, Astrophys. J.,**249**, 687.
- [34] Ostriker J.P., Gunn J.E., 1969, ApJ **157**, 1395
- [35] Manchester, R. ., Taylor, J. . 1977, Pulsars, W. . Freeman, San Francisco, pp.**121**, 188.
- [36] Goldreich P., Julian W.H., 1969, ApJ **157**, 869
- [37] Goldreich, P. 1970, Astrophys. J., **160**, L11.
- [38] Blandford R.D., Romani R.W., 1988, MNRAS **234**,57
- [39] Cheng A.F., 1989, ApJ**337**, 803
- [40] Muslimov A., Page D., 1996, ApJ **458**, 347
- [41] Blandford R.D., Applegate J.H., Hernquist L., 1983, MNRAS, **204**,1025
- [42] Camilo F., 1996, in IAU Colloquium 160, Pulsars: Problems and

Progress, Jonston S., Walker M.A., Bailes M. (eds.), ASP Conf.Ser. 106, San Francisco, 39

[43] Link B., Epstein R., 1997, ApJ **478**, L91

[44] Groth, . J. 1975, Astrophys. J. Suppl. Ser.,**29**, 453.

[45] Yakovlev ,D. G. , Gnedin, O. Y.,Kaminker, A. D. and Potekhin, A. Y., Theory of cooling neutron stars versus observations, AIP Conf. Proc.,**983** (2004) 379-387.

DECLARATION

I hereby declare that this thesis is my original work, has not been presented for a degree in an other university and that all the sources of material used for the thesis have been dully acknowledged.

Name: Selemawit mehari

Signature:.....

This thesis has been submitted for examination with my approval as university advisor.

Name: Dr.Legesse Wetro

Signature:.....

Place and time of submission:

Department of Physics
Addis Ababa University
June 2014